# DESIGN OF MEDICAL HIGH-VOLTAGE POWER SUPPLY BASED ON INTEGRAL SEPARATION PID CONTROL

Kaiyuan WEI[1], Yajun WANG[2]

*The traditional high-voltage power supply is mainly in oil-immersed type with open-loop design. Traditional HV power design leads to large volume, high output voltage ripple coefficient. A novel high-voltage power source design method based on integral separation PID control is proposed in this paper. The method establishes the mathematical model of DC HV power with closed loop control system, and the control scheme of integral separation is introduced in this method. When the deviation between the controlled quantity and the set value is larger, the integral action is canceled. However, when the controlled quantity is close to the set value, the integral control is introduced to eliminate the static error and improve the precision. The simulation results show that the high-voltage power supply based on integral separation PID control has small output voltage ripple and high stability, which can be used in medical high voltage equipment.*

**Keywords**: integral separation PID control; medical high-voltage power supply; high stability; closed-loop control.

## 1. Introduction

Some medical devices, such as laser surgical scalpels, can achieve surgical functions by the transition of electrons under high voltage. There are many kinds of laser scalpels, gas lasers, solid lasers, semiconductor lasers, and liquid lasers [1-3]. Taking a xenon gas laser as an example, high-voltage needs to be applied at both ends of the gas pipe to make the electron transition. The required high voltage is 23000V [4]. Because of the sophistication and importance of surgery, high-voltage power supply with high stability is required for its power source. Therefore, the stability of HV power has become an important index.

In recent years, the high-voltage source is mainly in oil-immersed type with open-loop design. Traditional HV power design leads to large volume, high output voltage ripple coefficient. It is not conducive to the use of medical equipment terminals. Considering the important role of the intelligent control to industrialization and high-intensity gas discharge lamp, a control type high

[1] Postgraduate, School of Electronic and Information Engineering, Liaoning University of Technology, China, e-mail: 344410622@qq.com

[2] Prof., School of Electronic and Information Engineering, Liaoning University of Technology, China, e-mail: wyj_lg@163.com

voltage power supply with small volume and low ripple coefficient of output voltage comes into being.

With the integration of electronic components, high-voltage DC source has made rapid development. PWM control-based high-voltage power supply has the advantages of small size, small output voltage ripple coefficient and light weight to transport [5-6]. In this paper, a novel high-voltage power supply design method based on integral separation PID control is proposed. The corresponding mathematical model is built. In the simulation environment of MATLAB, the overall circuit is simulated according to the characteristic of switching source.

## 2. Overall Program Design

The gas laser is powered by switched high-voltage power supplies. High-frequency square wave is produced by the inverter circuit. The adjustable range of duty cycle for the PWM waveform is 33%–50%. The signal is sent to the rectifier filter voltage-multiplying circuit through the high-frequency boost transformer, where the transformer ratio is 1:12. The voltage-multiplying circuit adopts Kockcroft-Walton circuit [7-8] which is also known as trapezoidal double voltage rectifier circuit. Thus, the DC high-voltage is produced. Then the output voltage is sampled and sent to the AD converter. The PWM wave is adjusted through the PID integral separation control algorithm to control the output voltage. The overall scheme diagram is shown in Fig. 1.

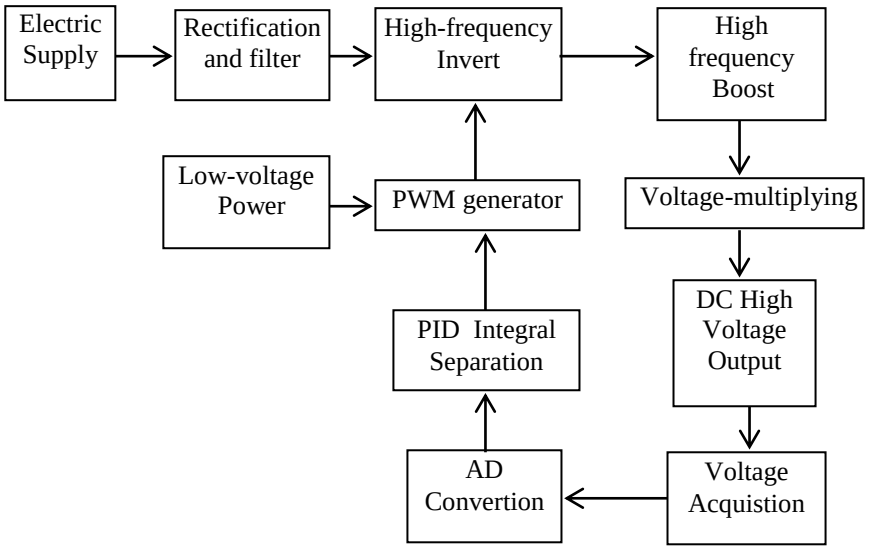


Fig. 1. Overall design scheme diagram

First, the DC 300V power source is obtained by the commercial power rectifier, which can supply electricity to the high-frequency inverter circuit. The PWM wave is adjusted to get adjustable high-frequency square wave. Then the high-frequency square wave is boosted by the transformer and output through the voltage-multiplying rectification circuit. The signal is controlled and adjusted by the integral separation PID controller after the sampling circuit and the AD conversion circuit. Finally, the stable DC high-voltage output is obtained. Specific circuit is shown in Fig. 2.

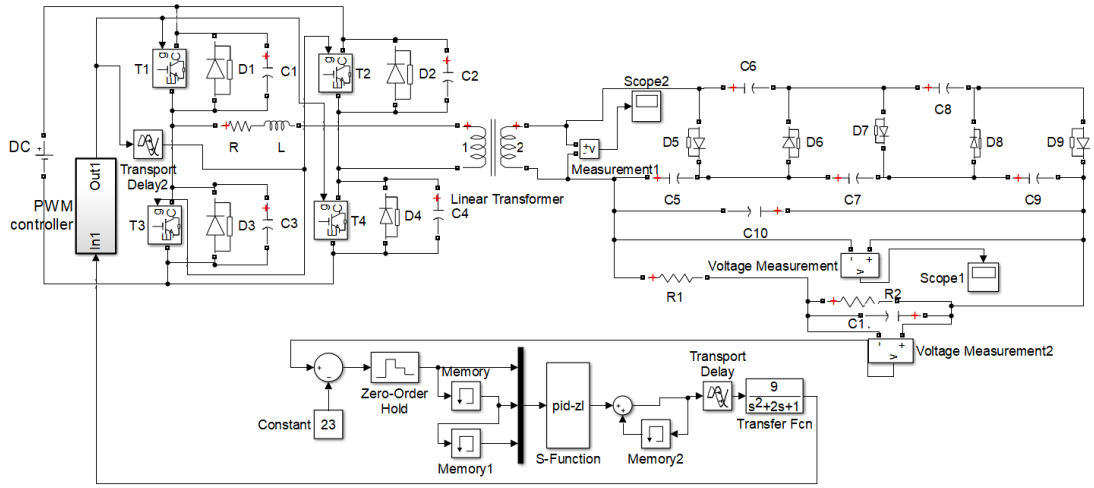


Fig. 2. Overall circuit

## 3. Analysis of the Overall Circuit Model

3.1 Inverter Circuit

Since the withstand voltage of IGBT is higher than that of MOSFET, the inverter circuit consists of four IGBTs. DC 300V voltage is inverted to high frequency square wave through the four IGBTs. The circuit diagram is shown in Fig. 3. The frequency of the square wave is 50kHz in this study.

Both IGBT and MOSFET can be used as a switch in the circuit. Since the switch operates at high voltage and high frequency, IGBT switch is chosen here.

The inverter under PWM control has a hysteresis, hence, it can be equivalent to an inertial link. Its transfer function [9] is:

$$W_1(s) = \frac{K_{pwm}}{Ts+1} \tag{1}$$

where $T$ is the PWM signal cycle. $K_{pwm}$ is the gain of the inverter. The gain can be obtained by equation (2).

$$K_{pwm} = \frac{E}{K_{lmt}} \tag{2}$$

where $E$ is the DC input voltage of the inverter, and $K_{lmt}$ is the output limiting value of the controller.

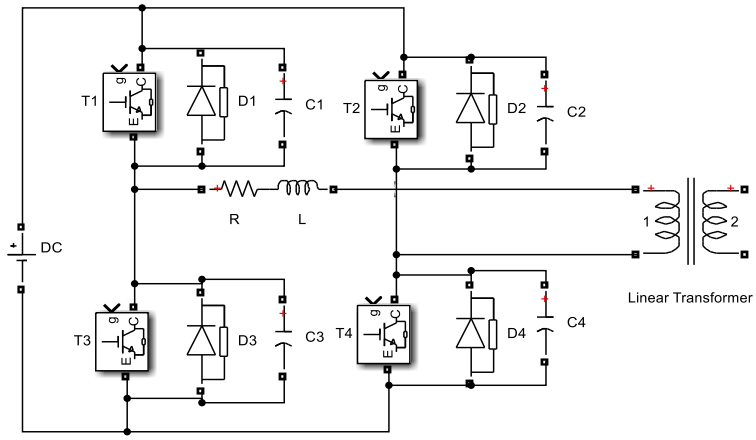


Fig. 3. Inverter circuit

In Fig. 3, $T_1$~$T_4$ are IGBTs, $D_1$~$D_4$ are anti-parallel diodes, and $L$ is the sum of series inductors and the equivalent inductance of the primary side of the transformer. Due to the presence of inductance, the output current lags the voltage with a certain angle.

When the driving signal is added to $T_1$ and $T_3$, the switching devices cannot be turned on immediately but freewheels through $D_1$ and $D_3$. The process is called forced commutation. In this case, the stored energy in the inductor decreases, and the absolute value of the load current decreases exponentially. When the load current crosses the zero point, the current is reversed and naturally shifted from $D_1$ and $D_3$ to the corresponding arm $T_1$ and $T_3$. This process is called natural commutation. Then the energy is transmitted from the current side to the load side until the next switch state changes. In the process of conversion between natural commutation and forced commutation, zero voltage switching (ZVS) can be achieved.

In actual circuit operation, switching devices are mostly operated under high current and high frequency conditions which may cause the bridge arm shoot-through phenomenon. At this point, if a certain voltage is applied across the

bridge arm, the inverter will be short. To avoid this phenomenon, the dead time is necessary to prevent the shoot-through phenomenon in a PWM (pulse-width-modulation) inverter feeding an induction motor. However, the dead time can reduce the system performance.

3.2 Design of High-frequency Transformer

The high frequency square wave from the inverter circuit is boosted by the transformer. The turns ratio of the transformer is set to 1:12. The transformer works at 50kHz. The rated current is 1A. The rated capacity is 5000Hz. And the rated power is 200VA.

The transfer function model of high frequency transformer is

$$W_2(s) = \frac{U_3(s)}{U_2(s)} = \frac{n^2 R_d}{(n^2 R_d + R_2 + n^2 R_3) + s(L_2 + n^2 L_3)} \tag{3}$$

where $R_2$, $L_2$ are the resistance and leakage inductance of the primary winding; $R_3$, $L_3$ is the resistance and leakage inductance of secondary winding; $R_d$ is the approximate resistive load; $n$ is the transformer ratio.

3.3 Voltage-multiplying Rectifier Circuit

In voltage-multiplying rectifier circuit, the voltage can be maintained at five times input voltage by rectification and guidance of capacitors and diode, and then they are connected together according to charge and discharge of the capacitor. Hence, the output is higher than the input voltage and the maximum output current can reach 10mA. The voltage-multiplying rectifier circuit is illustrated in Fig. 4 with five-voltage doubler. Electrolytic capacitors and high-voltage silicon reactor stack are used in circuit as a rectifier device.

In order to meet the miniaturization design requirements, dry high-voltage power supply generally adopts the modular structure. In accordance with the principle of high-voltage power supply and the function of various components, power source is divided into three modules: power distribution module, inverter module and high-voltage module. Power distribution module and inverter module only contain low potential. The high voltage module contains all high potential. Vacuum potting is used in high voltage module. This modular structure is simple and provides frequent power-on tests at any appropriate stage of manufacture and assembly in order to preserve the insulation of each module. Epoxy potting is chosen in high-voltage switch transformers. The modules are cooled through metal floor.

Voltage-multiplying rectifier circuit is a second-order system, the transfer function is:

$$W_3(s) = \frac{-m(s^2 + \omega^2)}{\omega s} \tag{4}$$

where m is the voltage-multiplying number of voltage-multiplying rectifier circuit; $\omega=2\pi f$ is the sinusoidal angular frequency.

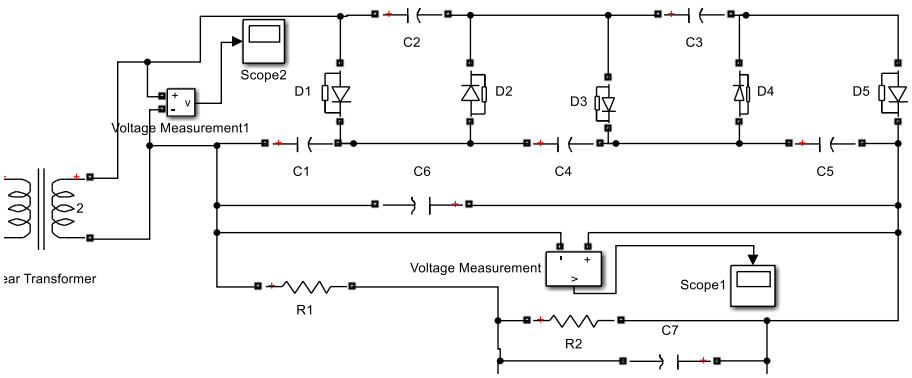


Fig.4. Voltage-multiplying rectifier circuit

## 4. Analysis and design of control loop

### *4.1 Establishment of Controller Model*

Loop detection control system block diagram is shown in Fig. 5. The output voltage is sampled by Hall sensor and sent to the controller. The sampled voltage is compared with the set voltage of 23000V, and the resulting error value is calculated by the processor to obtain the digital control value. Finally, the control amount is converted to the analog control amount U by the D/A converter and applied to the PWM controller so as to adjust the duty cycle of the PWM waveform and further control the output voltage so that the voltage is stabilized at around 23000V.

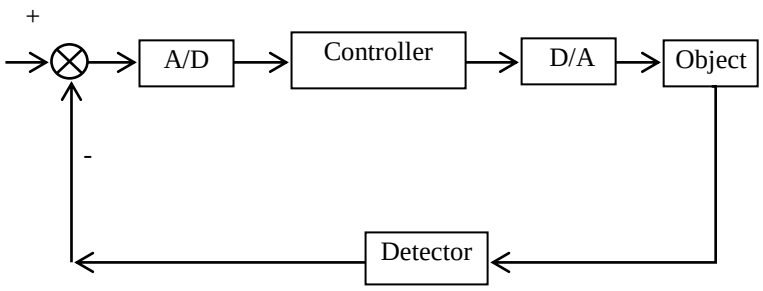


Fig. 5. Loop detection control system block diagram

Since the controller uses fixed-cycle sampling control, which is a discrete digital controller [10-11], Zero-order Hold is used in the simulation for input

sampling to achieve A/D conversion function. And the controller function involves loop control, condition judgment, operation logic and other operations, which cannot be described by the transfer function. Therefore, the s function (system function) and memory module are used in the simulation design. Since the controller relies on program instructions to complete the function, there is a delay in the input sampling and data processing. Hence the delay module is added to the simulation.

According to the characteristics of the controller above mentioned, the Simulink simulation is applied to establish the controller simulation model, as shown in Fig. 6.

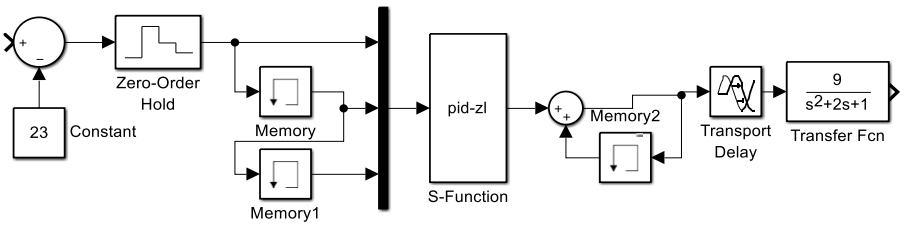


Fig. 6. Controller simulation model

The controlled object is a second order servo system, its transfer function is:

$$G(s) = \frac{9}{s^2 + 2s + 1} \tag{5}$$

### *4.2 Integral Separation Algorithm*

The introduction of integral in PID control can eliminate the static error and improve the control precision. However, in the process of starting, ending or large increase or decrease of the set value, the system outputs a large deviation in the short time, which will cause the integral accumulation of PID operation so that the control amount exceeds the maximum permissible range of action allowed by the executing agency. The system will cause larger overshoot, and even larger oscillations. This is not absolutely allowed in the control process [12].

In order to overcome the problem above discussed, the concept of integral separation is introduced. When the controlled amount deviates greatly from the set value, the integral action is canceled to avoid the decrease of the stability of the system, the increase of the overshoot, and larger oscillation due to the integral effect. When the controlled amount approaches the set value, the integral control is introduced to eliminate static error and enhance the precision. The integral PID control process is exhibited in Fig. 7. In Fig.7, $r$ is desired value, $y$ is output value,

and φ is threshold value. When the difference between *r* and *y* is higher than φ, the system cancels the integral function. Otherwise, the system introduces the integral function.

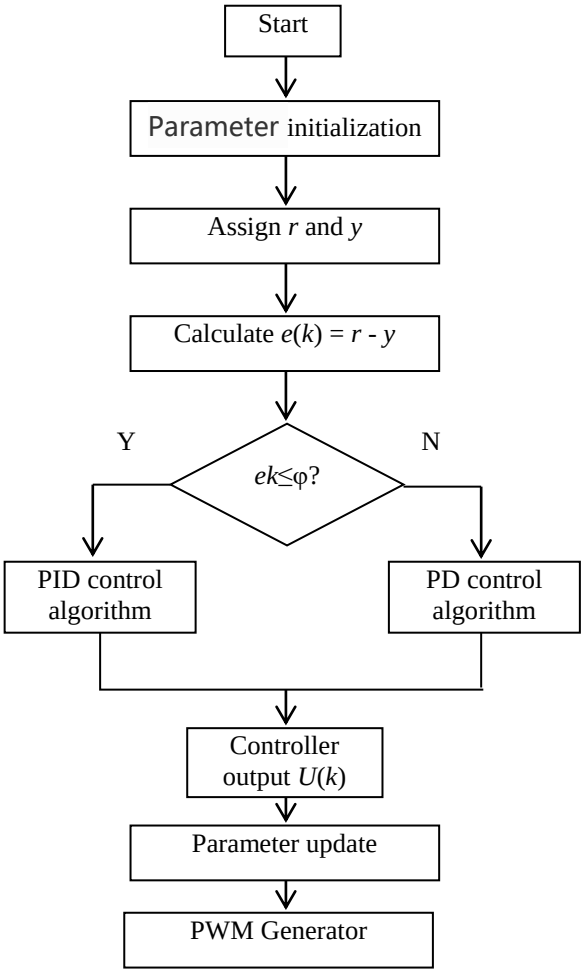


Fig. 7. Integral separation PID control algorithm flow chart

The specific algorithm [13-15] is as follows:

$$\Delta U(k) = K_p[e(k) - e(k-1)] + NK_i e(k) + K_d[e(k) - 2e(k-1) + e(k-2)]$$
$$N = \begin{cases} 1 & |e(k)| \le B \\ 0 & |e(k)| > B \end{cases} \tag{6}$$

where $\Delta U(k)$ is the increment of the control amount; $K_p$ , $K_i$ , $K_d$ are the proportional coefficient, integral coefficient and differential coefficient, respectively; $B$ is the error band. The position output of the PID controller is

$$U(k) = U(k-1) + \Delta U(k) \tag{7}$$

### *4.3 Parameter Determination*

(1) Determination of the proportional coefficient $K_p$

When the proportional coefficient $K_p$ is determined, the integral term and the differential term of the PID are first removed and then changed to pure proportional adjustment by setting $T_i = 0$ and $T_d = 0$. The input is set to 60 % to 70 % of the maximum allowable output of the system. The proportional coefficient $K_p$ gradually increases from 0 until the system oscillates. When the proportional coefficient $K_p$ gradually decreases from the current value until the system oscillation disappears, the result is recorded. Meanwhile, the proportional coefficient $K_p$ of the PID is set to 60 % to 70 % of the current value.

(2) Determination of the integral time constant $K_i$

After the proportional coefficient $K_p$ is determined, a large integral time constant $K_i$ is firstly set. $K_i$ then gradually decreases until the system oscillates. Followed by reverse operation, $K_i$ gradually increases until the system oscillation disappears. $K_i$ is recorded. The PID integration time constant $K_i$ is set to 150% to 180% of the current value.

(3) Determination of the differentiating time constant $K_d$

The differentiating time constant $K_d$ is generally not set. The value of $K_d$ is 0, then the PID adjustment is converted to PI adjustment. When $K_d$ is required, the determination process is the same as the method of $K_p$. Accordingly, $K_d$ is set to 30% of its value when system does not oscillate.

(4) No-load system simulink

PID parameters fine modulation is included until the performance requirements are met.

(5) Determination of $B$

a large integral time constant $B$ is firstly set. $B$ then gradually decreases until the system oscillates. Followed by reverse operation, $B$ gradually increases until the system oscillation disappears. $B$ is recorded. The Threshold value $B$ is set to50% to 80% of the current value.

Since the controlled object is a second-order system, the angular frequency $\omega_s$ of undamped natural oscillation is calculated as 10 $\omega_s$ , thus the sampling period of the system is $T=2\pi/\omega_s \approx 0.2$s. PID controller parameters $K_p$=0.6, $K_i$=0.4, $K_d$=1.5, and $B$=2.The memory has the function of storing the previous input value in Fig. 5, where Memory1 and Memory2 are used to store $e(k\text{-}1)$ and $e(k\text{-}2)$

respectively; Memory3 and the adder sum2 are used for realizing the position output of the controller.

## 5. Simulation Results

Under the condition of city electric power supply, Fig. 8 shows the secondary side waveform of the transformer after high frequency inversion. The measuring unit of X axe is second and Y axe is Volt. The frequency is 50 kHz. The duty cycle of the PWM signal is 44% after adjusting by the controller, and the voltage on the secondary side is 3193V, which accords with the transformer ratio setting of the transformer.

In Fig. 9, there is a surge voltage at the start of power-up due to the transformer leakage inductance. In the actual production process, electrostatic shield for the primary side coil is connected to ground. The ground of electrostatic shield must be a dedicated line from the power grounding bus. Meanwhile, the resistance should be connected in series with the ground wire. The resistance of the resistor is less than 10kΩ. High-frequency common mode noise and differential mode noise of 10-1000 kHz can be effectively suppressed by adding the capacitance filter circuit and the choke coil on the secondary side.

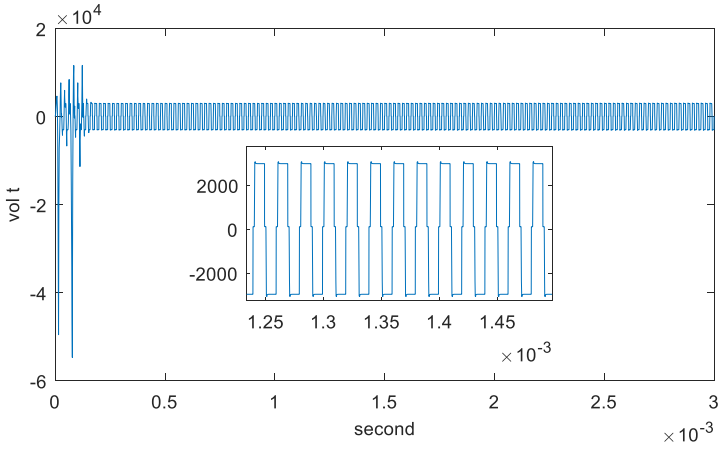


Fig. 8. The secondary voltage waveform of transformer

The designed system is applied to the laser generator. The invert high frequency square wave is rectified and filtered to output DC high-voltage. The output voltage is sampled to the processor with a 0.2s sampling period. The processor calculates the analog control value $U$ and sends it to the PWM controller to finely adjust the duty cycle of the PWM waveform so as to precisely control the output voltage. The measured DC high-voltage is 23030V, which is lower than 0.5% of the DC high-voltage pulse range. The measurements show that

the system meets the design requirements. The output waveform is shown in Fig. 9.

From the simulation results, output power of circuit is 70W. Inert gas laser input power is typically 30W, 35W, 50 W and 65W. The circuit is suitable for low power inert gas laser device.

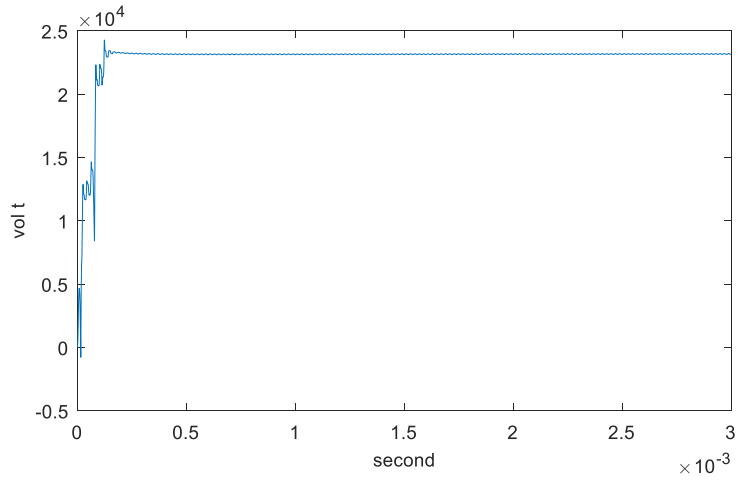


Fig. 9. DC high-voltage output waveform

## 6. Conclusions

The high-voltage power supply based on integral separation PID control has an adjustable range of duty ratio of 33% to 50%, and a high-voltage of 7000–30000V can be output in this range. Adopting the integral separation control strategy, the output voltage has high stability and small ripple. The error is up to 0.1%. It can be used on high precision laser scalpels and X-ray instruments, and can also be used on welding equipment and electrical equipment.

## R E F E R E N C E S

[1]. *Y. Xiang, Y.B. Chong, H.P. Liu and B. Zhu,* "Principle, Application and Research Progress of Medical Laser Therapeutical Device", in Chinese Medical Equipment J., **vol. 33**, no. 8, 2012, pp. 84-86

[2]. *J. Brown, W. Neuberger.* Radial medical laser delivery device: US, US5292320, 1994

[3]. *M. Iliescu, B. Comanesc and E. Nutu,* "Rapid prototyping use in manufacturing components of a medical laser device", in DAAAM international vienna., **vol. 45**, no. 5, 2008, pp. 23-28

[4]. *J.M. Sun, H. Takano, M. Nakaoka and DC Lin,* "Transformer parasitic high-frequency inverter-fed DC-DC converter for medical-use X-ray power generator and its digital control", in IEEE International Conference on Industrial Technology, 1997, pp. 400-405

[5]. *D.J Jackson, J.F Naber, R.T Jr, M.M Crain and K.M Walsh*, "Portable high-voltage power supply and electrochemical detection circuits for microchip capillary electrophoresis", in Analytical Chem., **vol. 75**, no. 14, 2003, pp. 3643-3649

[6]. *J.M. Alonso, J. Garcia, A. J. Calleja and J Ribas*, "Analysis, design, and experimentation of a high-voltage power supply for ozone generation based on current-fed parallel-resonant push-pull inverter", in IEEE Transactions on Industry Applications., **vol. 41**, no. 5, 2005, pp. 1364-1372

[7]. *J. Beerten and R. Belmans*, "Analysis of power sharing and voltage deviations in droop-controlled DC grids", in IEEE Transactions on Power systems., **vol. 28**, no. 4, 2013, pp. 4588-4597

[8]. *X. Bonnin, J. Brandelero, N. Videau, H. Piquet and T. Meynard*, "A High Voltage High Frequency Resonant Inverter for Supplying DBD Devices with Short Discharge Current Pulses", in IEEE Transactions on Power Electronics., **vol. 28**, no. 8, 2014, pp. 4261-4269

[9]. *A. Leon-Masich, H. Valderrama-Blavi, J. M. Bosque-Moncusi and J Maixe-Altes*, "Principle, Application and Research Progress of Medical Laser Therapeutical Device", in IEEE Transactions on Industrial Electronics., **vol. 62**, no. 1, 2015, pp. 229-237

[10]. *R. Oftadeh, M. M. Aref, R. Ghabcheloo and J. Mattila*, "Unified framework for rapid prototyping of Linux based real-time controllers with Matlab and Simulink", in Ieee/asme International Conference on Advanced Intelligent Mechatronics., 2012, pp. 274-279

[11]. *S. Nuratch*, "Firmware design and development of MCU and Matlab-Simulink interfacing for real-time measurement, analysis and control applications, International Conference on Electrical Engineering/electronics, Computer", in Telecommunications and Information Technology., 2016, pp. 1-6

[12]. *R. Patel, P. A. Bhoit and V. Sah*, "DSP based digital controller for high voltage SMPS", in International Conference on Information Communication and Embedded Systems., 2015, pp. 1-5

[13]. *L. Huang, Y.X. Yang, S.J. Shen, Z.L. Zhong, L.J. Zheng and P. Feng*, "Integral Separation PID Control in the Control of Lye Concentration", in Advanced Materials Research., no. 627, 2013, pp. 489-496

[14]. *Y. Furukawa and F. Kurokawa*, "Analytical approach for novel digital PID control switching power supply", in IEEE International Conference on Industrial Technology., 2015, pp. 2444-2449

[15]. *W. Azaiez, M. Chetoui and M. Aoun*, "Analytic approach to design PID controller for stabilizing fractional systems with time delay", in International Multi-Conference on Systems, Signals & Devices., 2015, pp. 1-7